

Time Resolved Spectroscopy of Water in the Infrared: New Data and Discussion

Robert Laenen, Konstantinos Simeonidis, and Alfred Laubereau*

Physik-Department E11, Technische Universität München, D-85748 Garching, Germany

(Received July 30, 2001)

We demonstrate sub-picosecond spectroscopy of an isotopic water mixture presenting strong evidence for four major spectral components within the OH-band of HDO in the solvent D_2O peaked at approximately 3330 cm^{-1} (I), 3390 cm^{-1} (II), 3460 cm^{-1} (III), and 3520 cm^{-1} (IV). Species I and IV are. proposed to give rise for discrete components with local hexagone and weakly bound structures, respectively. The remaining species are most probably related to combination tones with hydrogen bridge bond vibrations. Furthermore we summarise the findings on the vibrational and spectral dynamics of water as determined by time-resolved IR-spectroscopy of HDO molecules dissolved at low concentration in D_2O.

Water as the most important liquid exhibits special properties due to its ability to form a hydrogen-bonded network. The striking consequences for the biosphere are well known, e.g. the anomalous melting and boiling points of the liquid relative to similar molecules. For a detailed understanding numerous experimental and theoretical investigations were conducted on water.[1] The structure of water was examined by neutron[2] and X-ray[3] scattering while the reorientation of water molecules was studied by NMR[4] and dielectric relaxation[5] measurements. Recently the fast intermolecular motion has been elucidated by measurements on the sub-100 fs time scale using the Raman-induced Kerr effect.[6] Time-resolved laser spectroscopy with subpicosecond time resolution has opened the door for a detailed view on the vibrational and structural dynamics water, as recently has been summarised.[7]

As the hydrogen-bridge-bond vibrations themselves are up to now not directly accessible for pump-probe experiments, the OH-stretching mode has been utilized as an ultrafast spectroscopic probe.[8] The sensitivity of the mode to the hydrogen-bonding situation was exploited by conventional infrared[9,10] and Raman[11] spectroscopy in order to identify different structural components applying also temperature or pressure changes. In corresponding time-resolved experiments of water samples low concentrated HDO:D_2O solutions were investigated in order to overcome the complication by the three different vibrational transitions of protonated water with spectral overlap in the region around 3400 cm^{-1}. The first transient spectroscopy of the isotopic mixture HDO in D_2O delivered evidence for inhomogeneous broadening with distinct spectral components in the range 3340 cm^{-1} to 3520 cm^{-1} at room temperature.[12] Due to the limited time-resolution of 11-ps pulses the dynamics of the various components could not be measured. Subsequent investigation with shorter IR-pulses shed new light on the ultrashort time dynamics of water while some experimental results demonstrate the need for further investigations and a more objective and detailed discussion. In the following we start into this direction by presenting new results on the sub-picosecond spectroscopy of an HDO:D_2O sample. A comparison with the results obtained by the two other groups utilising time-resolved IR-spectroscopy is also attempted.

Experimental

Our experimental system was discussed in detail elsewhere[13] and is only briefly described here. We start with a pulsed, Kerr-lens modelocked Nd:YLF laser for the synchronous pumping of two optical parametric oscillators in parallel. Single-pulse selection, frequency down-conversion and amplification of the OPO outputs are carried out in subsequent optical parametric amplifiers (OPA's).[14] Independently tunable excitation pulses of $\geq$ 450 fs duration and spectral width $\leq$ 35 cm^{-1} are generated in the range 1600 to 3700 cm^{-1}, and similarly for the probe.[13] Special features are the separate, computer controlled tuning of the pump and probe frequency positions as well as the adjustable IR-pulse duration in the range 0.5 ps to 2.6 ps. Difference-frequency generation between an amplified laser pulse and one pulse out of the OPO pulse train results in shortest IR-pump pulses of 0.5 ps (spectral width 28 $\pm$ 3 cm^{-1}) in the whole accessible spectral range and 0.5 ps probe pulses (spectral width 34 $\pm$ 3 cm^{-1}).

Only the shortest pulse durations indicated above are applied and two-color pump-probe absorption spectroscopy is carried out with moderate pump energies of $\simeq$1 μJ and frequency settings within the full width of the OH-band, producing small depletions of the vibrational ground state of a few percent. Probing energies are reduced to a few nJ, three orders of magnitude below the energy of the excitation pulse. The energy transmission $T(\nu)$ of the probing pulse through the excited sample is measured for parallel ($\|$) and perpendicular ($\perp$) polarisation with respect to the linearly polarized pump and compared with the sample transmission $T_0(\nu)$ for blocked excitation beam. The resulting relative transmission changes $\ln(T/T_0)_{\|,\perp}$ for variable probe frequency ν and probe delay time t_D are used in the following as the relevant signal quantities, from which an isotropic signal amplitude, $\ln(T/T_0)_{is} = (\ln(T/T_0)_{\|} + 2\ln(T/T_0)_{\perp})/3$ and an anisotropic signal $\ln(T/T_0)_{anis} = \ln(T/T_0)_{\|} - \ln(T/T_0)_{\perp}$ is deduced.[15] The isotropic signal delivers information on the number density and transient level population of the

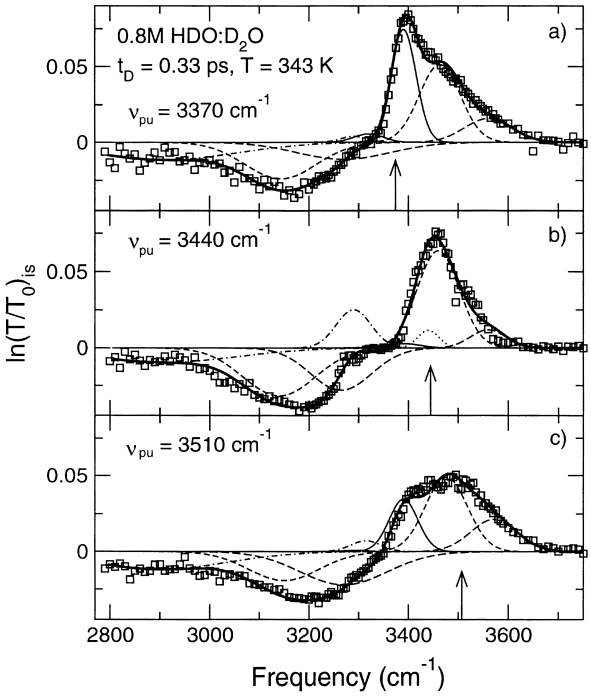

Fig. 1. Transient spectra of a 0.8 M HDO:D_2O solution taken at $t_D = 0.33$ ps and $T = 343$ K. The isotropic signal is plotted for three different pump frequencies: 3370 cm^{-1} (a), 3440 cm^{-1} (b), and 3510 cm^{-1} (c). Experimental hollow squares; the calculated thin lines indicate the analysis of the transient band-shapes (thick full line) in terms of the major spectral components I – IV (dash-dotted, thin solid, dashed, long-dashed) with Gaussian shape and a Lorentzian-shaped spectral hole contribution (dotted line); the pump frequencies are indicated by vertical arrows.

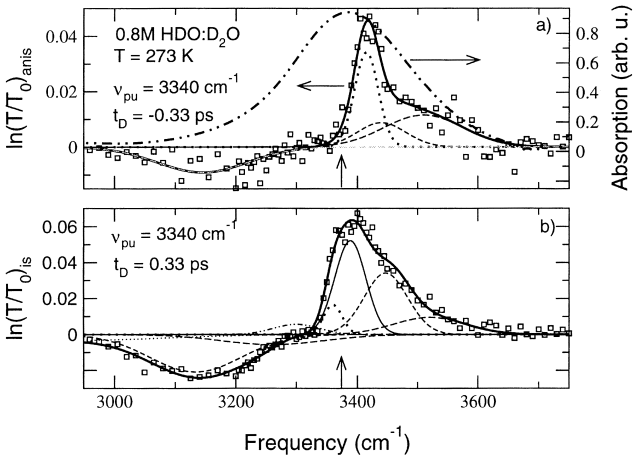

Fig. 2. Anisotropic data presenting clear evidence for spectral subcomponents underlying the broad OH-band of HDO are shown in (a) for excitation at 3340 cm^{-1} and $t_D = -0.33$ ps. The maximum bleaching is $\simeq$80 cm^{-1} blue-shifted in respect to ν_{Pu} (marked with an arrow). For comparison the conventional IR-absorption of the sample is depicted as dash-dot-dotted line and right hand ordinate scale. Isotropic data taken at the same excitation frequency (b) are also included similar to the one shown in Fig. 1, but this time taken at $T = 273$ K and $t_D = 0.33$ ps.

molecular species. The zero-setting of the delay time scale (maximum overlap between pump and probing pulses) is determined by a two-photon absorption technique in independent measurements with an accuracy of better than $\pm$0.2 ps.[16]

The sample solutions are prepared from commercially available deuterated water (99.9%) and tridistilled water without further purification. For HDO in D_2O a concentration of 0.8 M and a sample length of 100 μm are chosen, corresponding to a minimum sample transmission of 0.12 at 3400 cm^{-1} of the OH band ($T = 298$ K). The measurements are performed at two sample temperatures, 273 and 343 K.

To account for the rapid changes with delay time, the transient spectra are fitted by computed data assuming Gaussian shapes for the spectral components in general, while a possible spectral hole is considered to be Lorentzian. The Gaussian shape of the spectral lines accounts for an inhomogeneous broadening of the individual components due to for example variations in OH-bond lengths and angles. A contribution of homogeneous broadening to the individual spectral line width resulting in Voigt-profiles has been omitted. This is justified as within the measuring accuracy the data fitting procedure appeares to be not very sensitive to a certain amount of homogeneous broadening. The calculated spectra (solid lines) in Figs. 1 and 2 are the results of a fitting procedure using the Levenberg-Marquardt algorithm[17] for minimum deviations between the experimental points and the superposition of the spectral constituents. We note from our data that the spectral hole broadens in time due to spectral relaxation and this is also accounted for in the data analysis.

The signal transients are computed from a simplified rate equation model that is based on a 4-level system and takes into account the two orthogonal polarisations of the probing process.[18] The finite lifetime of the induced transition dipole moments is neglected here (dephasing time $T_2 \ll 1$ ps). Coherent contributions to the signal due to a population grating diffracting the pump into the probe direction (coherence peak artifact) are taken into account with a finite value of the phase relaxation time.[19] The 4-level scheme is depicted in Fig. 3 and considers the vibrational ground state of the OH-stretching mode (0), a joint first excited level $v = 1$ (1) of the respective spectral component(s) directly pumped by the excitation pulse, and population redistribution to an intermediate state (2) representing the other spectral components involved in the dynamics and grouped together in only one level. Energy redistribution between levels (1) and (2) is described by a time constant τ_s, while population decay out of levels (1) and (2) proceeds in our model to a thermally modified, long-lived ground state (3). Vibrational excitation of the sample leads to a delayed, small temperature and pressure increase of the interaction volume on the ps-time scale with a corresponding red-shift and broadening of the OH-band. This sample heating is dissipated lateron on a much longer time scale (relaxation of level (3)) compared to our observation interval. The redistribution time τ_s from level (1) to (2) is consistently attributed to spectral relaxation of the primarily excited molecules selected in their specific environment by the frequency position of the pump pulse. The reverse process (2) $\rightarrow$ (1) is included assuming detailed balance. A contribution of vibrational energy transfer among the HDO molecules appears to be negligible because of the small HDO concentration and the large frequency mismatch between solute and solvent modes. For the population decay of levels (1) and (2) to (3) the simplification $\tau_{13} \simeq \tau_{23} = T_1$ is introduced. The latter time constant denotes an av-

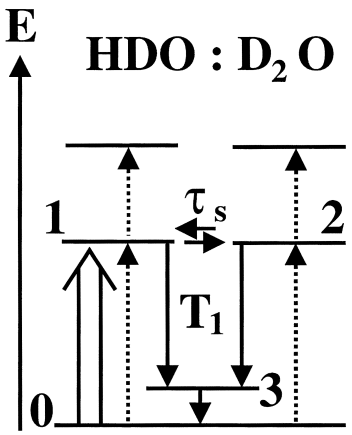

Fig. 3. Energy level scheme used for numerically fitting of the measured signal transients. Excitation (thick arrow) results in a population of level 1 with spectral relaxation to level 2 assuming detailed balance. Further relaxation proceeds via a hot ground state (3) back to level 0. Thin arrows denotes relaxation channels, dashed arrows possible probing transitions.

erage population lifetime of the OH-stretching mode of HDO.

Results

Transient spectra for three excitation frequencies within the bandwidth of the OH-stretching band of HDO in D_2O at a low concentration of 0.8 M are shown in Fig. 1. The isotropic component of the induced transmission change is plotted in order to focus on the population dynamics without a contribution of the reorientational motion of the transition dipoles. The spectra are taken at $t_D = 0.33$ ps for a sample temperature of 343 K. The measured spectral intensity distributions consist for the three denoted excitation frequencies of (i) a sample bleaching (positive signal amplitude) for probing frequencies above $\simeq$3350 cm^{-1} that is explained by the depletion of the ground state and population of the upper vibrational level. (ii) In addition, a red-shifted induced absorption occurs for $<$ 3350 cm^{-1} that is due to excited state population and the anharmonic frequency shift of probing a transition to a second excited level. In Fig. 1a with the lowest pump frequency of 3370 cm^{-1} (see vertical arrow) the bleaching band is notably asymmetric with an extended blue wing. The corresponding excited-state absorption (ESA) is structureless and peaks at 3180 cm^{-1}. Tuning ν_{pu} to 3440 cm^{-1} (Fig. 1b) yields a similar shift and more symmetric shape of the bleaching that is assigned to a dominant spectral sub-component of the OH-band close to the pump frequency position. Around 3320 cm^{-1} a plateau with vanishing signal amplitude is found that is explained by a compensation of bleaching and induced absorption components. Consequently the measured ESA bandshape is in this case considerably asymmetric with a steep wing around 3270 cm^{-1}. The striking differences of the bandshapes of Fig. 1 a and b directly reveal the pronounced inhomogeneous character of the OH band of HDO in heavy water.

The situation for a further increase of the pumping frequency to $\nu_{pu} = 3510$ cm^{-1} is shown in Fig. 1c. Here we find for the induced bleaching and absorption two broad spectral features centered at 3480 and 3220 cm^{-1}, respectively. The pronounced shoulder around 3410 cm^{-1} in the red wing of the bleaching band and the deviation between pump frequency and band maximum again point towards a more discrete substructure of the OH-vibration, i.e. spectral distribution function with multiple maxima. The experimental data are clearly inconsistent with a single-peaked, monotonicly rising and decaying frequency distribution. We also emphasize that a possible contribution of the coherence peak artifact to the transient bandshapes of Fig. 1a–c is insignificant at the stated delay time of 0.33 ps between pump and probe pulse. The latter would give an approximately Gaussian contribution with $\simeq$45 cm^{-1} width (FWHM) centered at the respective pump frequency, considerably narrower than the observed bleaching. Several factors combine to the small coherence peak amplitudes in our data (see below), as investigated recently.[19]

Similar transient spectra are recorded at 273 K and presented in Fig. 2. For comparison we have included in Fig. 2a the conventional IR-absorption of the sample (right hand ordinate scale, dash-dot-dotted line). This time the anisotropic (a) as well as the isotropic (b) signal components are plotted for delay times of -0.33 ps (a) and 0.33 ps (b), shortly before and after the maximum temporal overlap between pump and probing pulses, respectively. In Fig. 2a clear evidence for a discrete substructure of the OH-band of HDO is presented. The maximum bleaching with one dominant spectral component (dotted line) is noted $\simeq$80 cm^{-1} blue-shifted in comparison to the excitation frequency of 3340 cm^{-1}. This shift equals more than twice of the full spectral width of the two IR-pulses and can for this reason not be related to a simple coherent coupling artefact. An explanation of this spectral feature is most probably along the lines of a more complicated $\chi^{(3)}$–process involving stimulated emission into the probe branch which will be discussed into detail elsewhere.[20] This $\chi^{(3)}$–process results in a resonant enhancement of the stimulated emission into the probe direction due the presence of a distinct spectral component within the broad OH-band of HDO. The onset of vibrational population at this low excitation intensity is indicated in the figure by the broken lines (ground state bleaching) as well as the corresponding red-shifted excited-state absorption with respective small amplitude. One should note that in the discussed situation the probe pulse arrives notably before the maximum of the pump pulse at the sample.

Looking at the isotropic data taken at 0.33 ps we find for excitation at the same frequency of 3340 cm^{-1} (Fig. 2b) an asymmetric sample bleaching and broad structureless ESA. The shift of the bleaching peak relative to the pump frequency should be noted in the Figs. The band-shape is again assigned to a superposition of more than one spectral component involving also indirect excitation by fast spectral relaxation. A contribution of a spectral hole and/or coherent interaction is also inferred from the data analysis of Fig. 2b. For the present investigation with 0.5 ps-pulses and correspondingly poorer spectral resolution we are not able to distinguish here a spectral hole from other nonlinear interactions as different dynamics like vibrational and spectral relaxation proceeds on the same 1 ps-time scale. The visibility of the coherent signal contribution to the transient band-shape depends on the time delay of the pulses and obviously also on the dynamical properties of

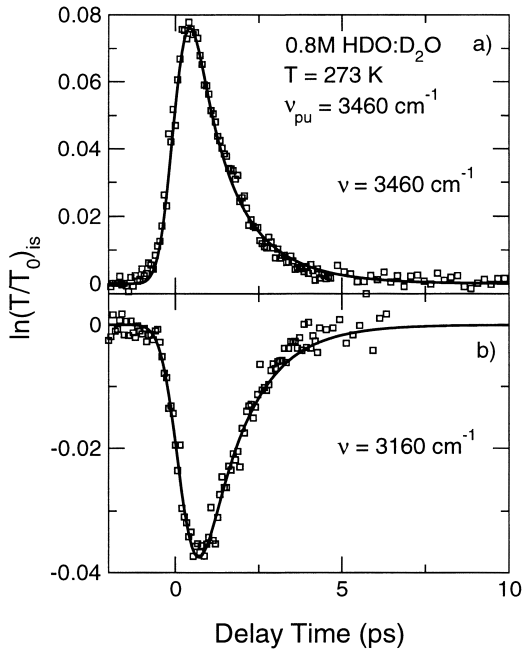

Fig. 4. The isotropic signal transients versus delay time at fixed probing frequencies and excitation at 3460 cm^{-1}, measured at $T = 273$ K: (a) sample bleaching for equal pump and probe frequency; (b) induced absorption probed at 3160 cm^{-1}; experimental hollow squares, calculated curves; a lifetime of the OH-stretching vibration of $T_1 = 1.2 \pm 0.3$ ps is obtained.

the individual spectral components. A deconvolution of the transient spectra by the help of a discrete set of spectral subbands is indicated in Figs. 1 and 2 by calculated curves with different line styles and will be discussed in the next section.

Examples for signal transients measured for fixed excitation at 3460 cm^{-1} and 2 different probing frequencies are depicted in Fig. 4. The isotropic signal is plotted for the 0.8 M HDO:D_2O sample at $T = 273$ K. Probing at the excitation frequency (Fig. 4a) we notice a transient bleaching that rises within the limit of temporal resolution of the apparatus while the subsequent decay is clearly resolved with a time constant of $\tau_{10} = 1.2 \pm 0.2$ ps describing repopulation of the vibrational ground state. A finite signal amplitude of 0.002 survives for $t_D \geq 10$ ps that is explained by a small heating of the excitation volume by the deposited pump energy. The generated excited state population in the $v = 1$ level(s) is directly monitored by probing at $\nu = 3160$ cm^{-1} (see Fig. 4b). Fitting calculated transients from our theoretical model mentioned above to the data an average lifetime of $T_1 = 1.2 \pm 0.2$ ps is inferred for the OH-mode of HDO in D_2O.

From comparison of the very small amplitude of the data probing the ground state population (Fig. 4a) at late delay times > 10 ps with temperature dependent conventional IR-spectroscopy we infer a local temperature increase by less than 1 K after excitation. This is due to the low pump energy of ≤ 1 μJ which is factor of 10 smaller compared to the one applied in similar studies by other groups.[21–23] For this reason the impact of the long lasting level (3) describing the locally heated sample is only very minor to the overall measured dynamics.

Vibrational and Structural Relaxation of the OH-Group

In order to provide detailed information from the measured transient spectra taken at (i) three excitation frequencies within the full width of the OH-band, (ii) at least 6 different delay time settings, and (iii) 2 sample temperatures of 273 K and 343 K, we consistently fit calculated transient spectra to the isotropic and anisotropic signal data for each sample temperature (data shown only in part). Four major spectral species are deduced from this procedure while the respective components show up in the measurements more or less clearly, depending on the sample temperature, ν_{Pu} and t_D (see for example Figs. 1 and 2). The spectral positions are 3330 (I), 3390 (II), 3460 (III), and 3520 cm^{-1} (IV) with a spectral width of respectively 80, 70, 80, and 140 cm^{-1}. The accuracy of the band positions and spectral widths is $\pm$ 20 cm^{-1} and $\pm$ 10 cm^{-1}, respectively. Only the amplitudes of the mentioned components are allowed to change with delay time and excitation frequency. A minor contribution denoted with I′ at 3270 cm^{-1} is also included for lower temperatures and excitation in the red wing of the OH-band. Further signal contributions of a spectral hole and/or coherent interaction are indicated in the figures by dotted curves. At early delay times $t_D < 0$ ps the transient spectra are strongly affected by coherent effects resulting in time-dependent positions and widths of spectral features located close to the excitation frequency. These findings will be subject of a separate publication as further investigations are needed for the interpretation.[20]

Data for the spectral reshaping described by the redistribution time τ_S are presented in Fig. 5 for excitation at 3460 cm^{-1} and a sample temperature of 273 K. The relative amplitudes (peak value of the isotropic signal) of species I to IV as obtained from the spectral decomposition of the respective transient spectra are plotted versus delay time. Data for $t_D < 0$ ps are omitted in the figure because of coherent signal contributions and spectral holeburning mentioned above. According to our theoretical model the resonantly pumped species III (open circles, dotted line) decays via two time constants, τ_S and T_1, the latter being known from the data of Fig. 4b while the initial fast decay is related to a spectral hole. Components I (hollow squares, dash-dotted line), II (hollow diamonds, solid line), and IV (hollow triangles, dashed line), on the other hand, are pumped by the excitation pulse only to a minor extent and grow up time delayed, obviously because of the spectral redistributrion process. Comparison with the rate equation model (calculated lines in the figure) yields the value $\tau_S = 1.5 \pm 0.5$ ps that is interpreted as the structural relaxation time of water at 273 K. Interestingly we include for component I also some coherent signal contribution around delay time 0, i.e. a temporal component which equals the cross-correlation between pump and probe and corresponds to some extend to the spectral features shown in Fig. 2a. A somewhat shorter number of $\tau_S = 0.8 \pm 0.4$ ps is deduced at 343 K (data not shown). The different spectral components seen in the ground state bleaching of the sample with respective temporal evolutions and peak positions are also reflected by corresponding species in the ESA. From the respective temporal evolution two components are seen in the ESA with peak at 3140 cm^{-1} and 3260 cm^{-1} which could tentatively be assigned to represent dominantly

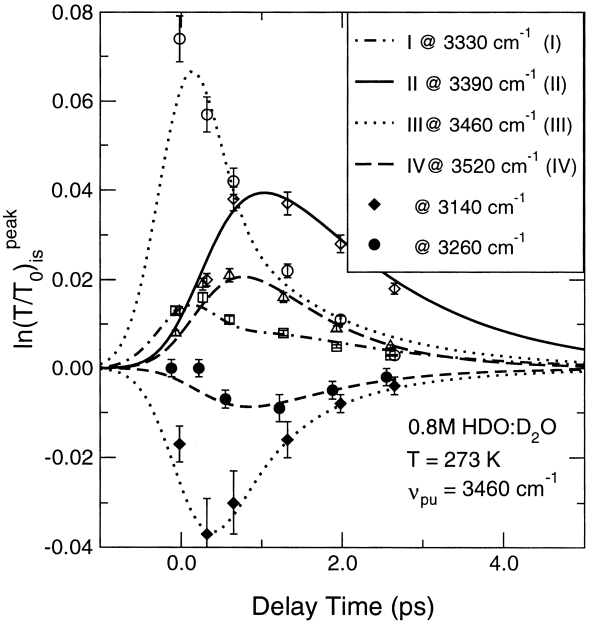

Fig. 5. Peak amplitudes of spectral components with assumed Gaussian shape versus delay time; the sub-bands fitted to the isotropic transient spectra measured for 273 K and $\nu_{pu} = 3460\ cm^{-1}$. The four major components I – IV in the sample bleaching denoted by different symbols and line styles are derived from fitting of a four level energy scheme to the data. A time constant for structural relaxation of 1.5 ± 0.5 ps is derived from the data. For comparison also the two ESA contributions are presented, denoted by the filled symbols.

transitions to the excited-states of components II and III, respectively. Due to the mixing of the OH-stretch with low frequency H-bridge bond vibrations (see next paragraphs) and the broader linewidths present in the excited-state absorption the spectral signatures seen clearly in the (0) → (1, 2)-transition are probably partly washed out.

Our finding for τ_S may be compared with results of computer simulations for water. Values between 1 ps to 2 ps are stated for the average lifetime of a hydrogen bond by different authors[24–26] in satisfactory agreement with our experimental value.

In a previous investigation[27] with somewhat longer pulses ($t_{Pu} = 2$ ps, $t_{Pr} = 1$ ps) we reported on three major spectral components with same values for the peak position and bandwidth of the sub-bands I and II within experimental accuracy. For a third component "III" a variable position of 3500 – 3450 cm^{-1} and width of 90 – 140 cm^{-1}, were found, changing notably with temperature (273 to 343 K). The analysis of the present data with improved time resolution suggests a simpler result: the former component "III" is to be replaced by two components III and IV with temperature independent positions and widths.

It is interesting to compare the widths and the frequency distance of the four major spectral components presented here with data from photon-echo studies[28] published recently on similar partly deuterated water samples. In the latter investigation a time constant for pure dephasing of about 100 fs is stated implying a dominant contribution of homogeneous broadening to the overall OH-line width. Nevertheless one should take into account the limited dynamic range of the photon-echo signal which could probably hinder the identification of recurrences of the signal previously[28] not noted. Photon-echo studies with extended dynamic ranges and probably shorter IR-pulses with corresponding broader spectra would be highly desirable to clarify into detail the homogeneous broadening of OH-bands in the presence of hydrogen bonds.

The presence of combination modes between the OH-stretch and low frequency H-bridge bond vibrations should result in a non-exponential decay of the induced sample bleaching. In the case of IR-pulses with bandwidths covering the different lines of the combination modes this could even lead to a beating in the signal. Recently Gallot et al.[29] reported on such a non-exponential decay of the ground-state recovery determined in a similar investigation. Here one has to recall that the bandwidth of 75 cm^{-1} of the utilised IR-pulses was not sufficient to cover the spectral lines discussed here completely.

We also mention that a further contribution to the transient spectra shows up in the induced absorption at $2940 \pm 20\ cm^{-1}$ (see Fig. 1) that is tentatively assigned to an overtone of the bending mode of HDO. A corresponding feature is found in the conventional IR-spectrum at $\simeq 2960\ cm^{-1}$. The observed induced absorption at this position presents some evidence that an excited level of the bending vibration is populated to some extend by energy transfer from the stretching mode. The relaxation channel was previously suggested for water vapor[31] and also proposed from time-resolved investigations[32,33] of a similar HDO sample. In the present study, the amplitudes of the mentioned component are too small to examine their temporal evolution with sufficient accuracy.

Our results on the spectral substructure of the OH-absorption are consistent with the band-shape in the conventional IR-spectrum of HDO. For a quantitative description of the latter the component I′ at 3270 cm^{-1} mentioned above is somewhat more important than in the transient spectra. A further contribution I″ to the conventional OH-absorption band of HDO is required at 3210 cm^{-1}. These additional contributions refer to the red wing of the OH-band $< 3300\ cm^{-1}$ where the resolution of the time-resolved technique is hindered by the superimposed excited state absorption. With the help of the mentioned spectral components we are able to nicely fit the OH-band of HDO in the temperature range of 273 – 343 K (data not shown).[30] From this fitting procedure we derive the following interdependencies: With rising temperature only species IV increases in peak amplitude, species III is almost constant while the other spectral components decrease in amplitude with approximately the same gradient. Taking furthermore the partly uniform temporal evolution of different pairs of the four spectral components (see for example Fig. 5) into account, we arrive at the following physical picture: Species I is located at a frequency close to the OH-frequency of HDO for the ice-structure I_h and is proposed to involve four strong, approximately straight H-bonds, as suggested by a comparison of the peak position with data of conventional infrared[34] and Raman spectroscopy.[35] The evidence for an approximately tetrahedral local geometry in liquid water in the measuring range 273 K to 343 K is in accordance with MD simulations.[36] Component II

with a similar temperature dependence is suggested to represent a combination tone[27,37,38] between the OH-mode and a low frequency H-bridge bond vibration of water molecules in the same local structure as I. For example the respective bending mode of the H-bond was determined from Raman spectroscopy[39] to be $\nu_b \simeq 50$ cm^{-1}. This nicely agrees with the frequency spacing of 60 ± 20 cm^{-1} between the spectral components I and II. The same argumentation holds for components I′ and I″, shifted again by $\simeq 60$ cm^{-1}. This assignment of spectral components of water to combination tones with bridge bond vibrations was already proposed previously.[12] The amplitude decrease of I and II with temperature is explained by a disappearance of the local tetrahedral structure and also by the thermal population redistribution among the low-frequency bridge bond vibrations.

The spectral component IV obviously corresponds to a notably weaker H-bonding situation and is tentatively assigned to molecules with bent or bifurcated H-bonds as concluded previously from MD-simulations[40] and Raman spectroscopy.[41] The assignment to a different local environment is supported by the notably shorter reorientation time.[21,27]

Our interpretation with two structural components I and IV do not exclude the existence of further local environments. It is recalled that in principle all of the twelve possible bonding configurations of HDO[42] may contribute to the overall OH-band with respective Raman-and/or IR-activity including the corresponding combination tones.

The decrease of sample transmission below 3300 cm^{-1} after excitation within the OH-band is clearly attributed to excited-state absorption (ESA) of probing transitions $v = 1 \rightarrow v = 2$. Two ESA components are derived from the transient spectra taken at different delay times. From the fitting procedure we obtain peak positions of 3140 cm^{-1} and 3260 cm^{-1} with respective widths of 170 and 200 cm^{-1}. The isotropic peak amplitudes of the two induced absorptions features are depicted versus delay time in Fig. 5 (filled diamonds and circles). Comparison of the temporal evolution and accounting for the frequency shift between $0 \rightarrow 1$ and excited-state transitions due to the anharmonicity of the OH-stretch suggestes the following result: the ESA peaked at 3140 cm^{-1} is related to the OH-mode of excited HDO molecules in the preferred local tetrahedral structure of components I and II with a vibrational lifetime of $T_1 = 1.2 \pm 0.4$ ps. The ESA with peak position of 3260 cm^{-1} displays vibrational excitation of the OH-stretch of weakly bound HDO molecules (species IV and perhaps III) with same population lifetime of 1.2 ± 0.3 ps within experimental accuracy. These numbers deduced from the data of Fig. 5 are in accordance with the more precise data of Fig. 4b. As the two time constants τ_{10} (including ground state recovery) and T_1 determined above from the signal transients of Fig. 4a and b are equal within measuring accuracy, there is no evidence for a long-lived intermediate state populated during the relaxation of the excited OH-stretch. As the dominant relaxation channel of the excited hydroxilic stretching vibration we tend to assign the excitation of low-frequency H-bridge bond vibrations because of the strong anharmonic coupling. This interpretation is in full accordance to the one recently proposed for H-bonded dimers[43] in liquid solution.

Discussion of the Published Time-Resolved Data on Water

Published results from time-resolved IR-spectroscopy of HDO:D_2O samples are summarised in Table 1. First we want to commment on the vibrational lifetimes of the OH-group of highly diluted HDO molecules in heavy water (first row in Table 1).

In our investigation we find typical numbers of 1 ps at room temperature and $\nu = \nu_{Pu} = 3410$ cm^{-1} and a trend to larger numbers for weaker H-bonds as present at higher frequencies within the OH-absorption. This principal trend is in agreement with data of Gale et al.,[32] however the lifetimes determined here are slightly longer in comparison to the numbers stated by those authors utilising the same experimental technique but working with shorter IR-pulses. Interestingly the stated numbers of T_1 are getting shorter with decreasing duration of the applied IR-pulses: Gale et al. mention at room temperature a value of 0.65 ps (3400 cm^{-1})[32] while no polarisation resolution was applied in the experiment, i.e. a mix up of the simultaneously measured vibrational and reorientational dynamics should result in a shorter apparent lifetime as reorientation proceeds on the same ps-time scale.[21] The Bakker's group resolves from an isotropic signal of a similar sample as discussed here $T_1 = 0.8$ ps,[22] closer to the numbers deduced from the present investigation. The obvious dependence of T_1 of water on the spectral width of the utilised IR-pulses should be subject to further investigations. We mention that our longer T_1 number cannot be simply related to a time-resolution problem since shorter lifetimes of 0.5 ± 0.1 ps are measured[44] by the same apparatus for crystalline ice.

The reorientational motion of the excited OH-dipoles was also investigated and the respective published numbers are listed in the second row of the table. From experiments conducted by two groups we find two typical time scales for this motion: our experiments[45] as well as the work[21] of the Bakker's group indicate for a slow reorientation with a 10 – 15 ps time constant for the stronger H-bonded OH-group as present in local tetrahedral structures (around 3300 – 3400 cm^{-1}) as well as fast motions for the weaker bonded HDO, seen in the blue part of the OH-spectrum with typically 1 – 3 ps. In contrast to this consistent picture in a later publication[23] the Bakker's group took the same data once more and interpreted them with the help of a quasi-continuous distribution of OH-oscillators in water.[46] Accourding to this later work the slower relaxing feature was attributed to stronger H-bonds present for the excited OH-groups in the $v = 1$ state.[23]

Finally we want to comment on the nature of the broadening of the OH-band of HDO due to the presence of H-bonds and the respective underlying dynamics. First evidence for a discrete substructure of the OH-band of HDO was demonstrated 1991 by Graener et al.[12] Due to the limited time-resolution of 11-ps pulses the dynamics of the various components could not be measured. Subsequent investigations with shorter and almost bandwidth-limited infrared pulses of 1 to 2 ps duration were able to substantiate the first findings and provided novel information on the spectral relaxation[45] among the different components in the temperature range 273 K to 343 K. The four species discussed here represent of an even more detailed picture which is now able to perfectly explain the temperature

Table 1. The Vibrational Lifetime T_1 of the OH-Stretching Vibration, the Time Constants for Spectral Relaxation (τ_S) and Reorientational Relaxation (τ_{or}) as well as the Experimental Conditions for the Various Time-Resolved Investigations of HDO:D_2O Samples Are Summarised Here (Discussion See Text)

HDO:D_2O	This work	Bakker's Group	Gale et al.
Population lifetime T_1	1.2 ± 0.2 ps (3460 cm^{-1}, 273 K) 1.0±0.2 ps (3410 cm^{-1}, 298 K) $T_{10} = T_{20}$	T_{20} = 0.74 ps (270 K)[22] T_{20} = 0.90 ps (298 K)[22] 3400 cm^{-1}, non-exp < 1 ps	0.5 ps (3270 cm^{-1})[32] 0.65 ps (3400 cm^{-1})[32] 1.0 ps (3600 cm^{-1})[32] $T_{10} = T_{20}$ 298 K, non-exp < 2 ps
Reorientation time τ_{or}	15 ± 5 ps (I, II, 273 K) 10 ± 3 ps (I, II, 289 K) 3 ± 1.5 ps (III, IV)[45]	13 ps (3320 cm^{-1})[21] 0.7 ps (3500 cm^{-1})[21] 2.6 ps (v = 0), 4.2 ps (v = 1)[23] 298 K	no polarisation resolution[32]
Spectral Substructure	quasi-discrete, 4 major species	continuous	continuous
Spectral dyanmics at 298 K	spectral relaxation τ_S = 1.0 ± 0.4 ps	dynamic Stokes shift[47] of 70 cm^{-1} τ_{eq} = 0.55 ± 0.05 ps[47]	spectral relaxation to band center with τ_Ω = 0.7 ps,[48] calculated with: T_1 = 1.3 ps, τ_{or} = 2.5 ps
t_P, $\Delta\nu$	500 fs, ≤ 35 cm^{-1}	250 fs, 90 cm^{-1}	150 fs, 65 cm^{-1}
ln (T/T_0)	< 0.1	< 0.3	?

dependence of the OH-absorption of HDO. The two preferred hydrogen bonded structures are supported by the different time scales of reorientation of the OH-group and theoretical approaches[40] to this problem.

Application of somewhat shorter IR-pulses in comparison to the present work with correspondingly poorer spectral resolution results in the following interpretation of the measured data: a time constant[47] of 0.55 ps was stated for spectral relaxation of the quasi-continuously distributed OH-oscillators together with a dynamic Stokes shift[47] of the OH-band. The latter observation is however in contradiction to measurements of Gale et al.[48] utilising even shorter 150 fs IR-pulses. The latter group derived from their data a continuous spectral relaxation to the band center with a longer time constant of 0.7 ps.[48] To determine this number the authors however considered values of T_1 = 1.3 ps and τ_{or} = 2.5 ps in their model calculations in order to fit their data.[48] These numbers for the prominent relaxation mechanisms are at variance with the respective numbers of the same group[32] but in well agreement to the OH-dynamics of HDO found by the present authors. As in the mentioned investigation[32] the parallel signal component of the probe transmission was measured, also the reorientational motion of the water molecules contributes to the measured dynamics.[21,45] A deconvolution of the various factors was not attempted in the data analysis. The notably broader spectra of the IR-pulses utilised in the experiments of Gale et al. as well as by the Bakker's group hinder to a large extent the determination of spectral holes and spectral substructures in the OH-band of HDO. Furthermore, only in our work and the one of Gale et al. transient spectra were presented, i.e. the continuous tunability of both IR-pulses pump and probe was fully utilised.

Conclusions

In this paper we present results of sub-picosecond IR-spectroscopy of HDO in the solvent D_2O. Our data measured at 273 K and 343 K confirm the physical picture developed in earlier investigations with somewhat longer pulses.[27] In the OH-band of HDO we identify 4 prominent spectral components I (3330 cm^{-1}), II (3390 cm^{-1}), III (3460 cm^{-1}), and IV (3520 cm^{-1}). From details of the transient spectra we conclude that the sub-bands represent physical reality and not just a parametrization of the band contours. Components I and IV represent most probably HDO molecules in two different environments: a local, approximately tetrahedral geometry (I) and a local structure with weak, angled hydrogen bonds (IV). Spectral components II and III are proposed to result from combination tones between the OH-stretch and a low-frequency H-bridge bond vibration (possibly bending mode), as supported by the temporal evolution of the respective spectral amplitudes: species II involving the local structure I, while component III may be related to a superposition of HDO molecules in environments I and IV. The interpretation is substantiated by a corresponding analysis of the temperature dependence of the conventional OH-band. The time constants reported in the present work fully confirm the ones reported previously.[27] The population decay time of the OH-mode is again measured to be T_1 = 1.0 ± 0.2 ps at room temperature. Structural relaxation between the prefered local structures proceeds with time constants of 1.5 ps (273 K) to 0.8 ps (343 K).

One of the authors (R. L.) is grateful to the Deutsche Forschungsgemeinschaft (DFG) for financial support.

References

1 F. Franks "Water, A Comprehensive Treatise," Plenum Press, New York, 1972.

2 J. Teixeira, M.-C. Bellissent-Funel, and S. H. Chen, *J. Phys. Condens. Matter*, **2**, SA105 (1990).

3 A. H. Narten and H. A. Levy in Ref. 1; T. Radnai and H. Ohtaki, *Mol. Phys.*, **87**, 103 (1996).

4 S. Meiboom, *J. Chem. Phys.*, **34**, 375 (1961).

5 J. Barthel, K. Bachhuber, R. Buchner, and H. Hetzenauer, *Chem. Phys. Lett.*, **165**, 369 (1990).

6 P. Foggi, M. Bellini, D. P. Kien, I. Vercuque, and R. Righini, *J. Phys. Chem. A*, **101**, 7029 (1997)

7 E. J. Heilweil, *Science*, **283**, 1467 (1999).

8 P. Schuster, G. Zundel, and C. Sandorfy, "The Hydrogen Bond, Vol. I–III," North-Holland, Amsterdam, 1976.

9 M. van Thiel, and E. D. Becker, G. C. Pimentel, *J. Chem. Phys.*, **27**, 486 (1957).

10 Y. Marechal, *J. Chem. Phys.*, **95**, 5565 (1991).

11 G. E. Walrafen, *J. Chem. Phys.*, **40**, 3249 (1964); G. E. Walrafen, *J. Chem. Phys.*, **47**, 114 (1967); G. E. Walrafen, *J. Phys. Chem.*, **94**, 2237 (1990).

12 H. Graener, G. Seifert, and A. Laubereau, *Phys. Rev. Lett.*, **66**, 2092 (1991).

13 R. Laenen, K. Simeonidis, and A. Laubereau, *J. Opt. Soc. Am. B*, **15**, 1213 (1998).

14 R. Laenen, K. Simeonidis, and C. Rauscher, *IEEE J. Selected Topics Quant. Electron.*, **2**, 487 (1996).

15 H. Graener, G. Seifert, and A. Laubereau, *Chem. Phys. Lett.*, **172**, 435 (1990).

16 C. Rauscher and R. Laenen, *J. Appl. Phys.*, **81**, 2818 (1997).

17 W. H. Press, B. P. Flannery, S. A. Teukolsky, and W. T. Vetterling, "Numerical Recipes," Cambridge University Press, Cambridge (1986).

18 Y. B. Band, *Phys. Rev.*, **A34**, 326 (1986).

19 R. Laenen and C. Rauscher, *Chem. Phys.*, **230**, 223 (1998).

20 R. Laenen, K. Simeonidis, and A. Laubereau, in preparation.

21 S. Woutersen, U. Emmeriches, and H. J. Bakker, *Science*, **278**, 658 (1997).

22 S. Woutersen, U. Emmeriches, H.-K. Nienhuys, and H. J. Bakker, *Phys. Rev. Lett.*, **81**, 1106 (1998).

23 H. -K. Nienhuys, R. A. van Santen, and H. J. Bakker, *J. Chem. Phys.*, **112**, 8487 (2000).

24 A. Geiger, P. Mausbach, J. Schnitker, R. L. Blumberg, and H. E. Stanley, *J. Phys.*, **45** C7, 13 (1984).

25 A. Luzar and D. Chandler, *Nature*, **379**, 55 (1996).

26 J. Marti, J. A. Padro, and E. Guardia, *J. Chem. Phys.*, **105**, 639 (1996).

27 R. Laenen, C. Rauscher, and A. Laubereau, *Phys. Rev. Lett.*, **80**, 2622 (1998).

28 J. Stenger, D. Madsen, P. Hamm, E. T. J. Nibbering, and T. Elsaesser, *Phys. Rev. Lett.*, **87**, 027401 (2001).

29 G. Gallot, N. Lascoux, G. M. Gale, J. -Cl. Leicknam, S. Bratos, and S. Pommeret, *Chem. Phys. Lett*, **341**, 535 (2001).

30 R. Laenen, K. Simeonidis, and A. Laubereau, *J. Phys. Chem. B*, **106**, 908 (2002).

31 J. Finzi, F. E. Hovis, V. N. Panfilov, P. Hess, and C. B. Moore, *J. Chem. Phys.*, **67**, 4053 (1977).

32 G. M. Gale, G. Gallot, and N. Lascoux, *Chem. Phys. Lett.*, **311**, 123 (1999).

33 J. C. Deak, S. T. Rhea, L. K. Iwaki, and D. D. Dlott, *J. Phys. Chem.*, **A104**, 4866 (2000).

34 T. A. Ford and M. Falk, *Can. J. Chem.*, **46**, 3579 (1968).

35 G. E. Walrafen, *J. Solut. Chem.*, **2**, 159 (1973).

36 F. H. Stillinger, *Science*, **209**, 451 (1980).

37 S. Bratos, *J. Chem. Phys.*, **63**, 3499 (1975); G. N. Robertson and Y. Yarwood, *Chem. Phys.*, **32**, 267 (1978); H. Abramczyk, *Chem. Phys.*, **144**, 305 (1990).

38 R. Laenen and K. Simeonidis, *Chem. Phys. Lett.*, **290**, 94 (1998).

39 G. E. Walrafen, M. S. Hokmabadi, and W.H.-Yang, *J. Phys. Chem.*, **92**, 2433 (1988).

40 F. Sciortino, A. Geiger, and H. E. Stanley, *Phys. Rev. Lett.*, **65**, 3452 (1990).

41 G. E. Walrafen, *J. Chem. Phys.*, **50**, 560 (1969).

42 E. C. W. Clarke and D. N. Glew, *Can. J. Chem.*, **50**, 1655 (1972).

43 R. Laenen and K. Simeonidis, *J. Phys. Chem.*, **A102**, 7207 (1998).

44 R. Laenen, K. Simeonidis, and A. Laubereau, *Laser Physics*, **9**, 234 (1999).

45 R. Laenen, C. Rauscher, and A. Laubereau, *J. Phys. Chem. B*, **102**, 9304 (1998).

46 S. Bratos and J. -Cl. Leicknam, *J. Chem. Phys.*, **101**, 4536 (1994).

47 S. Woutersen and H. J. Bakker, *Phys. Rev. Lett.*, **83**, 2077 (1999).

48 G. M. Gale, G. Gallot, F. Hache, N. Lascoux, S. Bratos, and J.-Cl. Leicknam, *Phys. Rev. Lett.*, **82**, 1068 (1999).